Life Sciences in Space Research 000 (2016) 1–7

Contents lists available at ScienceDirect

Life Sciences in Space Research

journal homepage: www.elsevier.com/locate/lssr

Solar proton exposure of an ICRU sphere within a complex structure part II: Ray-trace geometry

Tony C. Slaba[a,*], John W. Wilson[b], Francis F. Badavi[b], Brandon D. Reddell[c], Amir A. Bahadori[c]

[a] NASA Langley Research Center, Hampton, VA 23681-2199, USA
[b] Old Dominion University, Norfolk, VA 23529, USA
[c] NASA Johnson Space Center, Houston, TX 77004, USA

ARTICLE INFO

Article history:
Received 16 February 2016
Revised 29 April 2016
Accepted 9 May 2016
Available online xxx

Keywords:
Space radiation
Radiation shielding
Radiation transport
HZETRN

ABSTRACT

A computationally efficient 3DHZETRN code with enhanced neutron and light ion ($Z \leq 2$) propagation was recently developed for complex, inhomogeneous shield geometry described by combinatorial objects. Comparisons were made between 3DHZETRN results and Monte Carlo (MC) simulations at locations within the combinatorial geometry, and it was shown that 3DHZETRN agrees with the MC codes to the extent they agree with each other. In the present report, the 3DHZETRN code is extended to enable analysis in ray-trace geometry. This latest extension enables the code to be used within current engineering design practices utilizing fully detailed vehicle and habitat geometries. Through convergence testing, it is shown that fidelity in an actual shield geometry can be maintained in the discrete ray-trace description by systematically increasing the number of discrete rays used. It is also shown that this fidelity is carried into transport procedures and resulting exposure quantities without sacrificing computational efficiency.

Published by Elsevier Ltd on behalf of The Committee on Space Research (COSPAR).

1. Introduction

Primarily due to its high computational efficiency, the HZETRN code has been widely used throughout vehicle and habitat shield optimization activities, from preliminary architecture and trade studies through final design (Wilson et al., 2004a, 2004b; Qualls et al., 2001; Shavers et al., 2004) and as one element of multidisciplinary optimization software (Wilson et al., 2003). Further applications have been found in space environmental monitoring and validation (Hugger et al., 2003; Slaba et al., 2011a, 2013) and as a fundamental part of astronaut risk estimation for radiation safety monitoring (Cucinotta et al., 2008, 2013). Despite the broad applicability, one limitation of the HZETRN model is the use of the straight-ahead approximation wherein all particles are assumed to travel along a common axis. This approximation is known to be inaccurate for low energy neutrons and light ions ($Z \leq 2$) produced at broad angles relative to the incoming primary radiation.

Three-dimensional (3D) corrections to the HZETRN formalism for neutrons and light ions have recently been implemented, resulting in the 3DHZETRN code (Wilson et al., 2014, 2015a, 2015b). These improved transport procedures have been compared to state of the art Monte Carlo (MC) codes, Geant4 (Agostinelli et al., 2003), FLUKA (Fasso et al., 2005; Battistoni et al., 2007) and PHITS (Sato et al., 2006, 2013), using both simplified spherical geometry (Wilson et al., 2014, 2015a) and more complex combinatorial geometry configurations (Wilson et al., 2015b). In these benchmarks, it was generally concluded that 3DHZETRN agrees with the MC codes to the extent they agree with each other.

The 3DHZETRN code currently allows the improved transport procedures to be evaluated within general combinatorial geometry that may be defined in terms of solid objects (spheres, boxes, cylinders, ellipsoids) with unlimited nesting (i.e. objects within other objects). This capability was tested against MC simulations by considering a cylindrical outer shield with six internal objects, including a tissue sphere (Wilson et al., 2015b). Comparisons again showed that 3DHZETRN was in good agreement with the MC codes without sacrificing computational efficiency even in the more complex geometry considered.

In principle, the current capabilities of 3DHZETRN would support the broad range of design studies and risk assessment applications discussed at the beginning of this section. However, using only a limited set of combinatorial solids to describe realistic and highly complex vehicle designs, such as the International Space Station, with thousands of internal parts would likely lead to unnecessary approximations and related errors in the geometric

* Corresponding author. Tel.: +1 757 864 1420.
E-mail address: Tony.C.Slaba@nasa.gov (T.C. Slaba).

http://dx.doi.org/10.1016/j.lssr.2016.05.001
2214-5524/Published by Elsevier Ltd on behalf of The Committee on Space Research (COSPAR).

definitions. An alternative is to directly consider complex vehicle geometric descriptions typically developed in computer aided design (CAD) or finite element method (FEM) frameworks using ray-tracing methods. In such calculations, a ray-trace is performed over a large number of rays emanating from a target point within the geometry and extending outwards towards the exterior boundary. Along each ray, the length and type of each material traversed is stored. The resulting distribution of thicknesses is often referred to as a vehicle ray-trace or thickness distribution. Within the straight-ahead approximation of HZETRN, dosimetric quantities are quickly evaluated at the target point using either interpolation (Wilson et al., 1997) or ray-by-ray methods (Slaba et al., 2011b) coupled to the ray-trace geometry. A major advantage of this approach is that shield design is allowed to evolve in a more suitable CAD or FEM environment, instead of in the generally more restricted geometric definitions allowed by either MC transport codes or 3DHZETRN. In this work, the 3DHZETRN code is extended to allow evaluation within geometries defined simply by a vehicle thickness distribution file, referred to herein as a ray-trace geometry definition. This extension allows 3DHZETRN to be easily interfaced with methods based on CAD or FEM models that are already in common engineering practice. No modifications to the transport formalism are required for this extension of code capability. Only the ray-tracer used within 3DHZETRN along specific transport stream directions (Wilson et al., 2014) was modified.

To test this new capability, the combinatorial geometry studied previously by Wilson et al. (2015b) will be replaced by the corresponding ray-trace geometry definition evaluated at different target point locations (Wilson et al. 2015c). Convergence tests are performed on the number of rays used in the thickness distribution to evaluate the associated geometric discretization error. It is shown that more precise geometric representations and transport code solutions are achieved as the number of rays in the thickness distribution is increased, and the current practice of using $\sim 10^3$ rays may be sufficient in some cases. Results generated with 3DHZETRN from the ray-trace geometry are compared to 3DHZETRN results and MC simulations generated in the original combinatorial geometry (Wilson et al., 2015b). It is found that neither transport code accuracy nor efficiency is sacrificed with the extension to ray-trace geometry. This latest transport code advancement directly enables the use of more complex geometric models so that simple mapping of the present methodology into more realistic applications is achieved.

2. 3D transport through ray-trace geometry

In this section, the ray-tracer used in 3DHZETRN to estimate material types and thicknesses traversed through a ray-trace geometry definition is described. The transport formalism previously described by Wilson et al. (2014, 2015a, 2015b) is not altered. Fig. 1 shows a case in which the external radiation environment is assumed to impinge uniformly along the direction $\boldsymbol{\Omega}_0$ onto the geometry, and the solution is being evaluated at the point $\boldsymbol{x}$ along the stream direction $\boldsymbol{\Omega}$. Transport procedures require rapid evaluation of the materials and thicknesses traversed along an arbitrary direction extending from any point within the geometry to the outer boundary (along $-\boldsymbol{\Omega}_0$ from $\boldsymbol{x}_0$ in this example). Combinatorial geometry allows this evaluation to be performed analytically in closed form as described by Wilson et al. (2015b). In ray-trace geometry, the exact geometry specifications are replaced with a discrete set of unit ray directions, r_i, emanating from $\boldsymbol{x}$, along which only the thickness, $t_i^{(j)}$, and material types traversed by the ray are known. The superscript (j) is used here to denote that in complex geometry, there may be many distinct material types, appearing along a given ray, i.

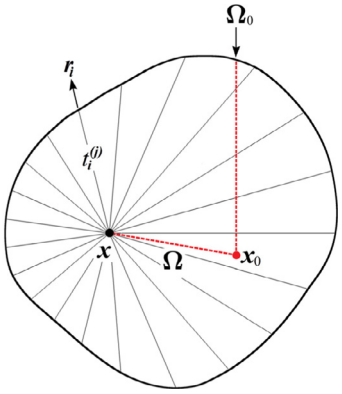

Fig. 1. General ray-trace geometry in which 3D transport procedures are evaluated.

In order to efficiently evaluate traversed materials and thicknesses through ray-trace geometry, some requirements need to be defined. First, to enable rapid searching through the distribution of rays used to define the ray-trace geometry, it is required that these rays be generated according to a latitude–longitude grid, as shown in Fig. 2. By using typical spherical coordinate transformations, the polar (longitude) and azimuthal (latitude) angles for each ray may be uniquely determined. The right side of Fig. 2 shows that these angles form a rectangular grid of points in two-dimensional space fully compatible with simple and efficient search algorithms used in bivariate interpolation. For an arbitrary ray-direction, its four nearest neighbors in the underlying ray distributions are easily found by simple search algorithms in two-dimensional space instead of computationally expensive comparisons against all ray directions in 3D space.

The only other requirement placed on the ray-trace evaluation mode is that at least one direction vector in the ray distribution must line up exactly with the incident direction of the incoming radiation environment, $\boldsymbol{\Omega}_0$. This requirement is implicitly required in existing engineering design practice already coupled to HZETRN in the straight-ahead approximation. The main reason for including this requirement in the ray-trace mode of 3DHZETRN is to ensure that evaluation of the forward flux component along $\boldsymbol{\Omega}_0$, which can dominate the overall exposure in many cases, is performed with precise geometric definition obtained directly from the native CAD or FEM geometry.

After satisfying these computational requirements, the ray-trace procedure carried out within 3DHZETRN for the ray-trace geometry is relatively simple. Consider the problem of ray-tracing from a point $\boldsymbol{x}_1$ along a direction $-\boldsymbol{\Omega}_0$, as shown in Fig. 3. To begin, the ray direction, $\boldsymbol{v}_1$ (green dashed line in figure) connecting $\boldsymbol{x}_1$ to $\boldsymbol{x}$ is constructed and the polar and azimuthal angles for $\boldsymbol{v}_1$ are computed. The four nearest neighbors of $\boldsymbol{v}_1$ in the underlying ray distribution are then determined by quickly searching the two dimensional (2D) grid of values shown in Fig. 2. In the 2D plot of Fig. 3, the visible neighbors are shown as blue solid lines. The closest of the neighbors, $\boldsymbol{r}_c$, is then selected, and the material type at a distance of $d_1 = |\boldsymbol{v}_1|$ along $\boldsymbol{r}_c$ is obtained directly from the ray-trace geometry file. This material type is assigned to the point $\boldsymbol{x}_1$. A step of 0.1 mm is then taken in the direction of $-\boldsymbol{\Omega}_0$ to define a new point, $\boldsymbol{x}_2$, and the process is repeated to determine the material type for point $\boldsymbol{x}_2$.

This process is repeated until the distance $d_n = |\boldsymbol{v}_n|$, where $\boldsymbol{v}_n$ is the ray connecting $\boldsymbol{x}_n$ to $\boldsymbol{x}$, and $\boldsymbol{x}_n$ is the point associated with step n in this procedure, is larger than the known distance along the nearest neighbor. This indicates that the outer boundary of the geometry has been reached. The end result of this procedure is a list of $\boldsymbol{n}$ material types corresponding to points spaced 0.1 mm part

Please cite this article as: T.C. Slaba et al., Solar proton exposure of an ICRU sphere within a complex structure part II: Ray-trace geometry Dochead is not present in PTS. Please check, Life Sciences in Space Research (2016), http://dx.doi.org/10.1016/j.lssr.2016.05.001